JOURNAL OF AIRCRAFT
Vol. 46, No. 6, November–December 2009

Fast Tool for Buckling Analysis and Optimization of Stiffened Panels

C. Bisagni* and R. Vescovini†
Politecnico di Milano, 20156 Milan, Italy

DOI: 10.2514/1.43396

This paper presents a fast tool that can be used during the preliminary design of isotropic and composite stiffened panels subjected to axial compression. It consists of two modules, one for the analysis and one for the optimization. The analysis is performed by implementing an analytical formulation to obtain the linearized buckling load and to study the nonlinear postbuckling field. In particular, closed-form solutions are derived for the linearized local and global buckling loads, and a semi-analytical procedure is implemented for the study of the nonlinear local postbuckling field. The optimization is based on genetic algorithms and allows taking into account buckling and postbuckling requirements with reduced computational time. Two examples regarding the minimum weight optimization of an isotropic panel and a composite panel are discussed and verified by means of finite element eigenvalue and nonlinear analyses. The total time required for the analysis and the optimization is of the order of a few minutes, and the difference between the analytical and numerical results is below 9% for the buckling load and below 3% for the postbuckling stiffness.

Nomenclature

$[A]$, $[B]$, $[D]$	=	membrane, coupling, and bending stiffness matrices of the skin
$[\bar{A}]$, $[\bar{B}]$, $[\bar{D}]$	=	membrane, coupling, and bending stiffness matrices of the smeared panel
A_{st}	=	stiffener cross-sectional area
a, B	=	panel length and width
$[a]$, $[b]$, $[d]$	=	semi-inverse relation matrices
b	=	distance between the stiffeners
E	=	Young's modulus for isotropic material
EA, EJ	=	axial and bending stiffness of the stiffeners
E_{11}, E_{22}	=	longitudinal and transverse Young's moduli for the composite ply
F	=	functional related to the panel
F_{sk}	=	functional related to the skin
f	=	objective function for the constrained problem
fit	=	fitness function
f_{un}	=	objective function for the unconstrained problem
G	=	shear modulus for isotropic material
GJ^*	=	half-torsional stiffness of the stiffeners
G_{12}	=	shear modulus for the composite ply
K_{pre}, K_{post}	=	prebuckling and postbuckling stiffness
$K_{\text{pre}}^{\text{ref}}$, $K_{\text{post}}^{\text{ref}}$	=	prebuckling and postbuckling stiffness reference value
$\{k\}$	=	vector of panel curvatures
$L_1(\,)$, $L_2(\,)$	=	differential operators
m, n	=	number of half-waves in longitudinal and transverse directions
N_c	=	number of constraints
N_{ik}, M_{ik}	=	forces and moments per unit length on the panel skin
$\tilde{N}_{ik}$, $\tilde{M}_{ik}$	=	forces and moments per unit length on the smeared stiffeners
$\bar{N}_{ik}$, $\bar{M}_{ik}$	=	forces and moments per unit length on the smeared panel
n_{st}	=	number of stiffeners
P, Q	=	number of terms for the out-of-plane displacement
P_{buck}	=	buckling load
$P_{\text{buck glob}}$	=	buckling load for global mode
$P_{\text{buck loc}}$	=	buckling load for local mode
$P_{\text{buck}}^{\text{ref}}$	=	reference buckling load
q_{mn}, q_{rs}	=	amplitudes of out-of-plane displacement for the $(P \times Q)$-term solution
q_1, q_2	=	amplitudes of out-of-plane displacement for the two-term solution
q_m^c	=	amplitudes of out-of-plane displacement satisfying clamped conditions
q_{mn}^{ss}	=	amplitudes of out-of-plane displacement satisfying simply supported conditions
R, S	=	number of terms for Airy stress function
S_1^C, S_2^C	=	longitudinal and transverse compression strength for the composite ply
S_1^T, S_2^T	=	longitudinal and transverse tensile strength for the composite ply
S_{12}	=	in-plane shear strength for the composite ply
T, U	=	number of terms for geometrical imperfections
t	=	skin thickness
t_{eq}	=	equivalent thickness of the smeared panel
t_{ply}	=	ply thickness
u, v	=	in-plane displacements
V_{sk}	=	skin total potential energy
V_{st}	=	stiffeners strain energy
W, W^{ref}	=	panel weight and reference panel weight
$w(x, y)$	=	out-of-plane displacement
$w_0(x, y)$	=	geometrical imperfection
X	=	vector of design variables
X_i, X_i^{ref}	=	design variable and design variable reference value
x, y	=	coordinates on the panel midsurface
$/x$, $/y$	=	partial differentiation with respect to the coordinates on the panel midsurface
$\bar{z}$	=	stiffener eccentricity

Presented as Paper 5978 at the 12th AIAA/ISSMO Multidisciplinary Analysis and Optimization Conference, Victoria, British Columbia, Canada, 10–12 September 2008; received 23 January 2009; revision received 6 June 2009; accepted for publication 23 June 2009.

*Associate Professor, Department of Aerospace Engineering, Via La Masa 34; chiara.bisagni@polimi.it. Member AIAA.

†Ph.D. Candidate, Department of Aerospace Engineering, Via La Masa 34, vescovini@aero.polimi.it.

γ_{ik} = shear strains
γ_{12}^{S} = in-plane shear strain limit for the composite ply
Δu = axial displacement
ΔX_i = nondimensional ith constraint violation
ϵ_{kk} = normal strains
$\epsilon_1^C, \epsilon_2^C$ = maximum longitudinal and transverse compressive strain for the composite ply
$\epsilon_1^T, \epsilon_2^T$ = maximum longitudinal and transverse tensile strain for the composite ply
η_i = penalty function
μ = amplitude of Airy stress function
ν = Poisson's ratio for isotropic material
ν_{12} = Poisson's ratio for the composite ply
$\xi_1, \xi_2, \xi_3,$ = nondimensional parameters
ρ = material density
σ = prebuckling stress
σ_{buck} = buckling stress
$\chi(x, y)$ = Airy stress function

I. Introduction

STIFFENED panels are common structural elements in aeronautical applications, and different strategies have been proposed in literature to obtain optimal designs even if there are often difficulties related with the ability to handle a high number of design variables and to describe the buckling and postbuckling behavior. For example, PANDA2 [1] is a program based on a gradient optimization algorithm for the minimum weight design of composite panels with or without stiffeners. It uses simple models to obtain prebuckling, buckling, and postbuckling responses under different loading conditions. VICONOPT is another program based on a stiffness matrix method with exact flat-plate theory and a gradient-based optimization strategy, used for the optimization of stiffened panels of an aircraft wing [2].

The main difficulties related to the use of gradient methods when dealing with composite structures is given by the fact that they can find points of local optimum and that the discrete variables, such as the number of plies and the orientation angles, have to be approximated as continuous variables. For this reason, genetic algorithms [3] have been widely used for the optimization of composite structures. They offer the possibility of handling discrete variables as well as of providing global optimization capabilities. For example, genetic algorithms were used by Nagendra et al.[4], considering stiffened composite panels under compression and shear loads. They also presented an improved version of genetic algorithms with reference to laminated structures [5], by introducing new operators and obtaining better convergence performances. In a few cases, genetic algorithms have been used together with the finite element method. An example can be found in the work of Kang and Kim [6], in which genetic algorithms are coupled with the finite element method to perform minimum weight analysis of unstiffened and stiffened composite panels with buckling and postbuckling constraints, and parallel computing techniques are applied to reduce the CPU time. Faggiani and Falzon [7] optimized stiffened panels using genetic algorithms and the finite element methodology, taking into account damage resistance within the postbuckling regime.

The high computational effort is the main limitation of the use of genetic algorithms together with the finite element analysis. This justifies the interest for more time-effective strategies, for which the main idea is to replace the finite element method with approximation techniques. Bisagni and Lanzi [8] presented an optimization for the minimum weight design of stiffened composite panels subjected to buckling and postbuckling constraints using genetic algorithms and neural networks trained by means of finite element analyses to reduce the computational costs. Other global approximations methods, such as radial basis functions and kriging, were used in a multi-objective optimization based on genetic algorithms presented by Lanzi and Giavotto [9], and surrogate models built employing the response surface method were presented by Rikards et al. [10]. An application of genetic algorithms together with analytical and numerical methods can be found in the work of Herencia et al. [11] within the context of a two-level optimization, in which membrane and flexural anisotropy is taken into account, and constraints regarding buckling are introduced referring only to a linearized analysis. Jaunky et al. [12] presented a minimum weight optimization strategy for grid-stiffened panels based on genetic algorithms and analytical formulations, always with the constraints limited to the linearized buckling load.

The use of an analytical approach results in an attractive strategy due to its effectiveness in terms of computational time, especially if compared with conventional numerical procedures such as the finite element method. This aspect becomes even more important when dealing with highly nonlinear analyses and in the context of optimization procedures, in which repeated analyses are required. With respect to the finite element method, which can analyze arbitrary geometry, load, and boundary condition, the analytical approaches are generally restricted to simplified conditions, such as the first buckling mode exhibited by the structure.

In the case of global buckling load (i.e., the buckling with half-waves encompassing several stiffeners), which is typical of closely spaced and not-too-stiff stiffeners, the analytical formulations usually refer to the so-called linear smeared theory. It is based on the idea of smearing the stiffeners over the panel, so that the stiffeners are distributed over the panel and are considered as an additional layup to the panel skin. The linear smeared theory is discussed in several papers, with applications to isotropic panels [13] and orthotropic panels [14,15].

Several analytical approaches can be found in the literature in the case of local buckling load (i.e., the skin buckling between the stiffeners), which is the typical buckling mode of the aeronautical stiffened panels. A common approach is to consider a null or an infinite amount of restraint given by the stiffeners to the panel edges rotations, so that the study of the stiffened panel can be conducted on a plate with clamped or simply supported boundary conditions. Under these assumptions, classical closed-form solutions are available for both isotropic [16] and composite panels [17]. This approach was applied, for example, by Pevzner et al. [18] to study the local buckling load of a composite cylindrical stiffened panel, in which the portion of skin between the stiffeners is assumed to be simply supported along the longitudinal direction and clamped along the circumferential direction. Paik and Thayamballi [19] presented a strategy to take into account the amount of restraint to edge rotations given by the stiffeners. They considered an isotropic stiffened panel that is modeled as a panel elastically restrained along the edges. The equilibrium equation were then solved using the method of Kantorovich, and closed-form solutions were also derived. Another approach that enables taking into account the interaction between skin and stiffeners is that presented by Fujikubo and Yao [20]. They derived a closed-form solution for the linear buckling load of isotropic stiffened panels, modeling both skin and stiffeners as plates, thus allowing the possibility of also considering local web buckling. The problem was solved using energy principles and applying the method of Ritz with appropriate shape functions. An analogous approach was presented by Mittelstedt [21] in the case of composite materials.

In any case, all these analytical formulations deal with the study of the linearized buckling load. On the other hand, more recent analytical formulations regard the study of nonlinear postbuckling field, considering the case of local buckling. A semi-analytical formulation for the study of the local postbuckling field of isotropic stiffened panels was discussed in the work of Byklum and Amdahl [22], considering a plate model for both skin and stiffeners and applying the large-deflection-plate theory. Buermann et al. [23] extended the analysis to the case of cylindrical isotropic panels, also including frames and doublers. The formulations for the postbuckling field of stiffened panels made of composite materials are even more rare. Mentioned among them is the work of Romeo and Frulla [24], in which the POBUCK computer program, based on a semi-analytical approach, is presented. The case of stiffened anisotropic panels subjected to biaxial loading was analyzed, and the local postbuckling analysis was performed considering the stiffeners as simply

supported and clamped boundary conditions. A simplified analysis for the nonlinear postbuckling of simply supported composite panels was presented by Bisagni [25] and closed-form solutions were derived. Sheinman and Frostig [26] presented a semi-analytical formulation for the postbuckling analysis of composite stiffened panels, modeling the panel as a plate assembly.

It is finally noted that all the works cited so far deal with longitudinally stiffeners. Skewed stiffeners have been proposed to obtain axial-shear stiffness coupling and to improve structural performance, as done by Young et al. [27]. However, this configuration is not considered here.

The goal of this work is to present a fast tool for the analysis and the optimization of longitudinally stiffened panels subjected to axial compression. Buckling and postbuckling constraints, such as those on the postbuckling stiffness, are handled in a fast way, and a numerical approach is not required. To this aim, an analytical formulation is developed, allowing for the study of the global and local buckling loads and local postbuckling field. The stiffeners are modeled as de Saint-Venant torsion bars, giving a better representation of the boundary conditions than in the case of idealized simply supported and clamped conditions.

The fast tool is obtained by coupling the analysis module, based on the analytical formulation, with an optimization module, based on genetic algorithms, as sketched in Fig. 1. The tool, implemented in C + + language program, performs a call from the analysis to the optimization module when the buckling and postbuckling behavior of a panel needs to be evaluated. The analyses are performed using the analytical formulation, and the results are sent back to the optimization module.

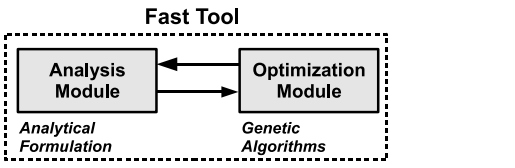

Fig. 1 Fast tool.

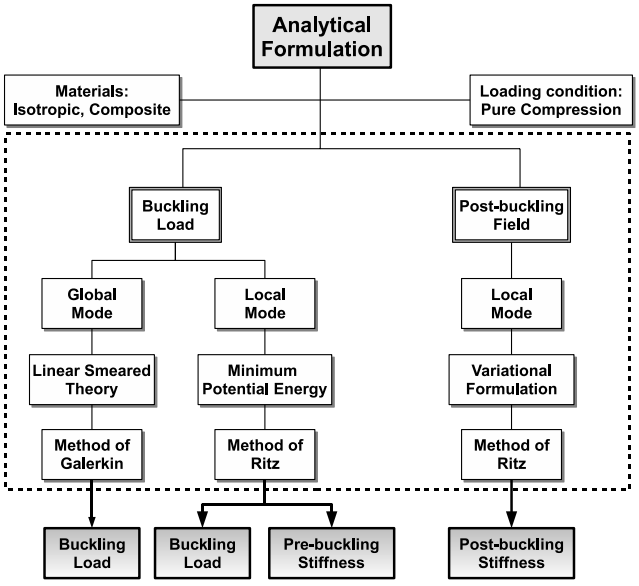

Fig. 2 Analytical formulation.

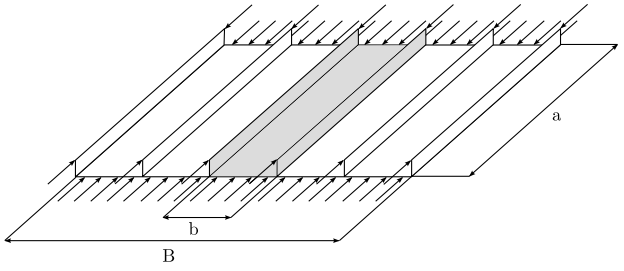

Fig. 3 Stiffened panel subjected to axial compression.

II. Analysis Module

The analytical formulation implemented in the analysis module is summarized in Fig. 2.

The formulation allows studying the elastic buckling load and postbuckling field of flat isotropic and composite panels with equally spaced longitudinal stiffeners subjected to pure compression load. A sketch of the analyzed panels is shown in Fig. 3, and the reference system and the positive directions of displacements, rotations, forces, and moments are reported in Fig. 4.

The analytical formulation allows obtaining the buckling load in the case of global and local buckling modes and the postbuckling field behavior in the case of only local buckling. This is motivated by the fact that aeronautical structures are generally designed to avoid global buckling as the first buckling mode. After the buckling, the structure can still carry loads until the collapse. In general, the ratio between the collapse load and the buckling load depends on the buckling mode exhibited by the structure. If the panel undergoes a global buckling mode, then the collapse load is generally close to the buckling load. On the other hand, when the buckling mode is local, the collapse load is much higher than the buckling load. In this case, the structure is generally allowed to work in the postbuckling field to obtain structural weight reduction.

The analytical formulation developed here is based on von Kármán [16] thin-plate theory, in which the transverse shear deformations are neglected. Isotropic and composite materials are considered. In the case of composite materials, the classical lamination theory is applied, introducing the hypothesis of symmetric laminate. The hypothesis of null bending-twisting coupling (i.e., $D_{16} = D_{26} = 0$) is also introduced in the linearized formulations for the study of local and global buckling loads. Moreover, in the case of global buckling, it is assumed that membrane anisotropy is null (i.e., $A_{16} = A_{26} = 0$).

The buckling loads are evaluated by means of two closed-form solutions for global and local buckling modes. In the case of global

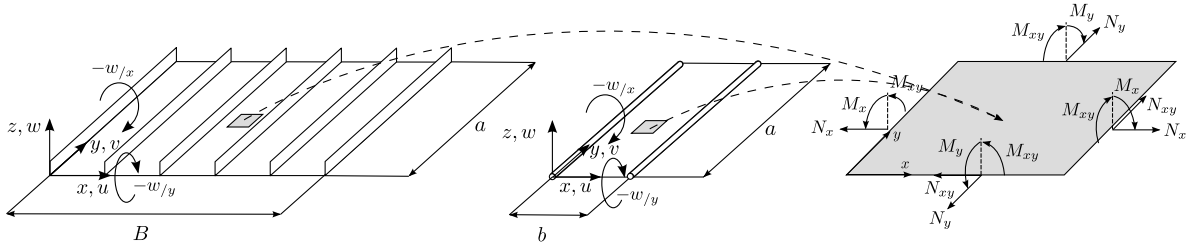

Fig. 4 Conventions for the analytical formulation: panel reference system, displacements and rotations for global buckling (left) and local buckling (center), and membrane forces and moments (right).

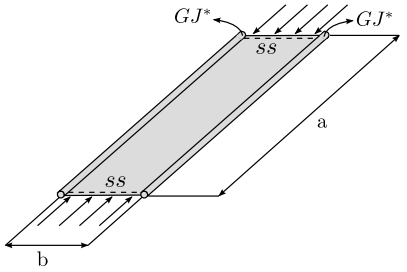

Fig. 5 Stiffened panel model for local buckling analysis.

buckling mode, the panel is studied referring to the linear smeared theory [13–15] and assuming simply supported conditions along all four edges. The equilibrium and compatibility equations are then solved by means of the method of Galerkin, obtaining a closed-form solution for the linearized buckling load.

In the case of local buckling mode, the panel is studied considering the skin between two stiffeners, which is chosen as a representative unit of the whole panel, as shown in Fig. 5. The stiffeners are not smeared onto the plate, but are considered as discrete entities, for which the torsional stiffness is taken into account, modeling the stiffeners as de Saint-Venant torsion bars. The panel is assumed to be simply supported along the loaded edges and elastically restrained along the longitudinal edges. The equilibrium is imposed applying the minimum potential energy principle, which is solved using the method of Ritz. A closed-form solution is obtained, which allows evaluating the buckling load also considering the contribute to the restraint of the edges rotation given by the stiffeners.

The study of the local postbuckling field is carried out modeling the panel as in the case of the local buckling load, thus considering the part of the panel between two torsion bars representing the stiffeners. The nonlinear problem is then formulated starting from a variational principle, in which the unknowns are the out-of-plane displacement and the Airy stress function. The nonlinear governing equations are derived introducing appropriate sets of trigonometric shape functions and applying the method of Ritz. As few terms of shape functions are usually sufficient to obtain accurate solutions, the nonlinear problem can be solved with a reduced computational effort.

A. Global Buckling Load

The analytical formulation for the study of the global buckling mode is presented here, obtaining a closed-form solution for the linearized buckling load. The theory is developed writing the governing differential equations that are solved using the method of Galerkin.

The linear smeared theory is applied, considering the stiffeners elastic properties averaged over the stiffener spacing and obtaining a panel with an additional layup of the skin due to the presence of the stiffeners. A Cartesian orthogonal coordinate system is taken over the panel midsurface, with the origin in the lower left corner of the panel, the x axis directed along the panel length, and the y axis along the panel width. The contribution to the smeared panel global stiffness is due to the stiffener axial and bending stiffnesses, and the torsional stiffness is not introduced into the model.

The additional layer due to the smearing process of the stiffeners is characterized by a distributed bending stiffness given by EJ/b, and a distributed axial stiffness given by EA/b. As a stiffener is generally characterized by an eccentricity $\bar{z}$, which corresponds to the distance between the skin midsurface and the stringer elastic centroid, the membrane force on the smeared layup can be written as

$$\tilde{N}_{xx} = \frac{EA}{b}(\epsilon_{xx} - \bar{z}w_{/xx}) \tag{1}$$

assuming that the strains vary linearly across the stiffener height, and satisfying the compatibility of displacements between skin and stiffeners.

Similarly, the bending moment acting on the smeared layup is

$$\tilde{M}_{xx} = \frac{EA}{b}\bar{z}(\epsilon_{xx} - \bar{z}w_{/xx}) - \frac{EJ}{b}w_{/xx} \tag{2}$$

The total forces and bending moments per unit length acting on the smeared panel are obtained by summing the terms related to the skin and the terms related to the smeared stiffeners. The forces per unit length are given by

$$\bar{N}_{ik} = N_{ik} + \tilde{N}_{ik} \tag{3}$$

where $i, k = x, y$. Similarly, the moments per unit length are written as

$$\bar{M}_{ik} = M_{ik} + \tilde{M}_{ik} \tag{4}$$

where $i, k = x, y$. From Eqs. (1) and (2) it can be seen that the presence of the longitudinal stiffeners affects only the terms $\tilde{N}_{xx}$ and $\tilde{M}_{xx}$.

Having defined forces and moments per unit length acting on the smeared panel by Eqs. (3) and (4), the equilibrium equations of the smeared panel are given by

$$\begin{cases} \bar{N}_{xx/x} + \bar{N}_{xy/y} = 0 \\ \bar{N}_{xy/x} + \bar{N}_{yy/y} = 0 \\ \bar{N}_{xx}w_{/xx} + \bar{N}_{yy}w_{/yy} + 2\bar{N}_{xy}w_{/xy} + \bar{M}_{xx/xx} + 2\bar{M}_{xy/xy} + \bar{M}_{yy/yy} = 0 \end{cases} \tag{5}$$

where the only difference with respect to the unstiffened panel relies on the presence of the distributed stiffnesses given by Eqs. (1) and (2).

The Airy stress function $\chi(x, y)$ is now introduced. It is related to the internal forces per unit length of the smeared panel. In the case of pure compressive load, the following is obtained:

$$\bar{N}_{xx} = -\sigma t_{\text{eq}} + \chi_{/yy} \qquad \bar{N}_{yy} = \chi_{/xx} \qquad \bar{N}_{xy} = -\chi_{/xy} \tag{6}$$

where the prestress σ is taken positive in compression, and t_{eq} is the equivalent thickness of the smeared panel, which is given by

$$t_{\text{eq}} = A_{\text{st}}/b + t \tag{7}$$

Substituting Eq. (6) into the equilibrium equations given by Eq. (5), the two in-plane equations are identically satisfied, and the out-of-plane equation is rewritten as

$$\begin{aligned} &-\sigma t_{\text{eq}}w_{/xx} + \chi_{/yy}w_{/xx} + \chi_{/xx}w_{/yy} - 2\chi_{/xy}w_{/xy} \\ &\quad + \bar{M}_{xx/xx} + 2\bar{M}_{xy/xy} + \bar{M}_{yy/yy} = 0 \end{aligned} \tag{8}$$

Having introduced the Airy stress function, the compatibility of displacements must be guaranteed. In this case, the compatibility equation, expressed in term of strains and considering only linear terms, is given by

$$\epsilon_{xx/yy} + \epsilon_{yy/xx} = \gamma_{xy/xy} \tag{9}$$

The governing equations (8) and (9) have to be rewritten in terms of the out-of-plane displacement w and the Airy stress function χ that are the unknowns of the problem.

The further assumption of null membrane anisotropy (i.e., $A_{16} = A_{26} = 0$) is introduced to simplify the derivation of a closed-form solution. Applying the classical lamination theory and considering Eqs. (1) and (2), the forces and moments per unit length acting on the smeared panel are related to the skin midsurface strains and curvatures by

$$\begin{Bmatrix} \bar{N}_{xx} \\ \bar{N}_{yy} \\ \bar{N}_{xy} \\ \bar{M}_{xx} \\ \bar{M}_{yy} \\ \bar{M}_{xy} \end{Bmatrix} = \begin{bmatrix} \frac{EA}{b} + A_{11} & A_{12} & 0 & \bar{z}\frac{EA}{b} & 0 & 0 \\ A_{12} & A_{22} & 0 & 0 & 0 & 0 \\ 0 & 0 & A_{66} & 0 & 0 & 0 \\ \bar{z}\frac{EA}{b} & 0 & 0 & \bar{z}\frac{EA}{b} + \frac{EJ}{b} + D_{11} & D_{12} & 0 \\ 0 & 0 & 0 & D_{12} & D_{22} & 0 \\ 0 & 0 & 0 & 0 & 0 & D_{66} \end{bmatrix} \begin{Bmatrix} \epsilon_x \\ \epsilon_y \\ \gamma_{xy} \\ -w_{xx} \\ -w_{yy} \\ -2w_{xy} \end{Bmatrix} \tag{10}$$

which can be rewritten in a more compact form as

$$\begin{Bmatrix} \{\bar{N}\} \\ \{\bar{M}\} \end{Bmatrix} = \begin{bmatrix} [\bar{A}] & [\bar{B}] \\ [\bar{B}] & [\bar{D}] \end{bmatrix} \begin{Bmatrix} \{\epsilon\} \\ \{k\} \end{Bmatrix} \tag{11}$$

From Eq. (11), the semi-inverse relation can be derived:

$$\begin{Bmatrix} \{\epsilon\} \\ \{\bar{M}\} \end{Bmatrix} = \begin{bmatrix} [a] & -[b]^T \\ [b] & [d] \end{bmatrix} \begin{Bmatrix} \{\bar{N}\} \\ \{k\} \end{Bmatrix} \tag{12}$$

where

$$[a] = [\bar{A}]^{-1} \qquad [b] = [\bar{B}][\bar{A}]^{-1} \qquad [d] = [\bar{D}] - [\bar{B}][\bar{A}]^{-1}[\bar{B}] \tag{13}$$

The strains and the moments per unit length can also be expressed in terms of forces per unit length and curvatures, and from Eq. (6) in terms of χ and w.

Substituting Eq. (12) into Eqs. (8) and (9), the equilibrium and compatibility equations can be written as

$$\begin{cases} L_1(\chi, w) = 0 \\ L_2(\chi, w) = 0 \end{cases} \tag{14}$$

where

$$L_1(\chi, w) = \sigma t_{\text{eq}} w_{/xx} + \chi_{yy} w_{/xx} + \chi_{xx} w_{/yy} - 2\chi_{xy} w_{/xy} + b_{12}\chi_{/xxxx} + b_{11}\chi_{/xxyy} - d_{11} w_{/xxxx} - (2d_{12} + 4d_{66}) w_{/xxyy} - d_{22} w_{/yyyy} \tag{15}$$

$$L_2(\chi, w) = a_{11}\chi_{/yyyy} + (2a_{12} + a_{66})\chi_{/xxyy} + a_{22}\chi_{/xxxx} + b_{12} w_{/xxxx} + b_{11} w_{/xxyy} \tag{16}$$

The unknown functions $w(x, y)$ and $\chi(x, y)$ are expressed using a one-term trigonometric series function:

$$w(x, y) = q \sin\frac{m\pi x}{a} \sin\frac{n\pi y}{B} \qquad \chi(x, y) = \mu \sin\frac{m\pi x}{a} \sin\frac{n\pi y}{B} \tag{17}$$

It is observed that the out-of-plane displacement identically satisfies the simply supported boundary conditions along the four edges.

The system of partial differential equations given by Eq. (14) is solved using the method of Galerkin:

$$\begin{cases} \int_0^a \int_0^B L_1(\chi, w) \sin\frac{m\pi x}{a} \sin\frac{n\pi y}{B} \, \mathrm{d}x \, \mathrm{d}y = 0 \\ \int_0^a \int_0^B L_2(\chi, w) \sin\frac{m\pi x}{a} \sin\frac{n\pi y}{B} \, \mathrm{d}x \, \mathrm{d}y = 0 \end{cases} \tag{18}$$

After some algebraic manipulations, a closed-form solution for the critical buckling stress of the smeared panel is derived:

$$\sigma_{\text{buck}} = \frac{1}{t_{\text{eq}}} \left(\frac{a}{m\pi}\right)^2 \left\{ \frac{[(m\pi/a)^4 b_{12} + (m\pi/a)^2 (n\pi/B)^2 b_{11}]^2}{[(m\pi/a)^4 a_{22} + (m\pi/a)^2 (n\pi/B)^2 (2a_{12} + a_{66}) + (n\pi/B)^4 a_{11}]} + \left[\left(\frac{m\pi}{a}\right)^4 d_{11} + \left(\frac{m\pi}{a}\right)^2 \left(\frac{n\pi}{B}\right)^2 (2d_{12} + 4d_{66}) + \left(\frac{n\pi}{B}\right)^4 d_{22} \right] \right\} \tag{19}$$

The obtained closed-form solution is a function of the unknown number of half-waves in longitudinal and transverse directions m and n. The buckling stress can be obtained by evaluating Eq. (19) for a sufficient number of (m, n) terms and taking the minimum value. The corresponding buckling load is easily derived multiplying Eq. (19) by the total cross-sectional area of the panel.

The obtained closed-form solution is compared with the one for global buckling of flat stiffened panels made of isotropic material reported in the appendix of [14]. The two formulations present two main differences. First, the solution reported in [14] is derived using the three components of the displacement as unknowns, and Eq. (19) is obtained using the out-of-plane displacement and the Airy stress function. Second, the stiffener torsional stiffness is accounted for in the solution proposed in [14], whereas it is neglected in Eq. (19).

The two equations are applied to obtain the buckling stress of a series of isotropic panels. The considered material is an aluminum alloy for which the mechanical properties are reported in Table 1. The number of stiffeners is taken equal to 5, the panel width is 700 mm, and the stiffener height is 28 mm. Figure 6 reports the normalized buckling stress versus the ratio between web and skin thickness for five different panel aspect ratios. The results show very good agreement between the two formulations. It can also be noted that the effect of neglecting the torsional stiffness does not influence the results.

B. Skin Local Buckling Load

The analytical formulation for the study of the local skin buckling is developed considering a representative unit of the panel, constituted by the portion of structure between two stiffeners, as shown in Fig. 5. The loaded edges are assumed to be simply supported, and the unloaded longitudinal edges are assumed to be elastically restrained by de Saint-Venant torsion bars, as done by the authors in a previous work [28].

The problem is formulated by writing the total potential energy of the structure, which is composed of two terms. The first one is associated with skin deflection, and the second term is due to the torsion of the stiffeners. The strain energy due to the skin deflection can be written as

$$V_{\text{sk}} = \frac{1}{2} \int_0^a \int_0^b (-\sigma t w_{/x}^2 + D_{11} w_{/xx}^2 + 2D_{12} w_{/xx} w_{/yy} + D_{22} w_{/yy}^2 + 4D_{66} w_{/xy}^2) \, \mathrm{d}x \, \mathrm{d}y \tag{20}$$

The strain energy associated with the stiffeners is given by

$$V_{\text{st}} = \frac{1}{2} \int_0^a GJ^* w_{/xy}^2 \, \mathrm{d}x|_{y=0} + \frac{1}{2} \int_0^a GJ^* w_{/xy}^2 \, \mathrm{d}x|_{y=b} \tag{21}$$

Table 1 Aluminum alloy mechanical properties

Material properties	Aluminum alloy
Young's modulus E, N/mm^2	72,400
Shear modulus G, N/mm^2	27,218
Poisson's ratio ν	0.33
Density ρ, kg/m^3	2,768
Yield stress σ_0, N/mm^2	340

as the rotation of the torsion bars is equal to the twist angle of the panel edge. Only half of the stringer torsional stiffness, indicated by GJ^*, is used to take into account the presence of adjacent structure [19]. The problem is solved using the method of Ritz and choosing appropriate shape functions. The elastic restraint can be considered as an intermediate condition between the simply supported and the clamped condition. The out-of-plane displacement can be represented as the superposition of two terms satisfying simply supported and clamped conditions:

$$w(x,y)=\left[q_1\sin\frac{\pi y}{b}+\frac{q_2}{2}\left(1-\cos\frac{2\pi y}{b}\right)\right]\sin\frac{m\pi x}{a} \tag{22}$$

The natural conditions of equilibrium between torsional moments along the stiffener axis and bending moments along the panel edges are given by

$$\begin{aligned} D_{22}w_{/yy}(x,b)&=GJ^*w_{/xxy}(x,b)\\ D_{22}w_{/yy}(x,0)&=-GJ^*w_{/xxy}(x,0)\end{aligned} \tag{23}$$

Only one of the two conditions needs to be imposed, because of the assumed symmetry of the function given by Eq. (22). Substituting Eq. (22) into Eq. (23), the unknown q_2 can be expressed in terms of q_1, and the expression of the out-of-plane displacement that identically satisfies the natural conditions given by Eq. (23) is obtained as

$$w(x,y)=q_1\left[\sin\frac{\pi y}{b}+\left(1-\cos\frac{2\pi y}{b}\right)\frac{GJ^*}{4D_{22}}b\pi\left(\frac{m}{a}\right)^2\right] \tag{24}$$

The equilibrium is imposed by applying the minimum potential energy principle:

$$\frac{\partial(V_{\text{sk}}+V_{\text{st}})}{\partial q_1}=0 \tag{25}$$

Substituting Eq. (24) in Eqs. (20) and (21) and applying Eq. (25), the following is obtained after some algebraic manipulation:

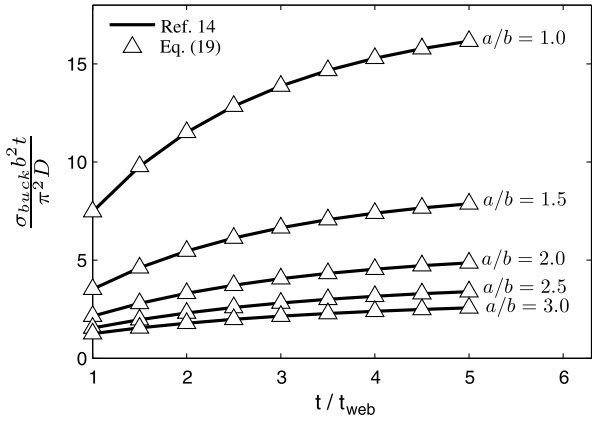

Fig. 6 Normalized buckling stress: comparison between Eq. (19) and the solution of [14].

$$\begin{aligned}&\left[\frac{b\pi^4m^4D_{11}}{12a^3}\left(3+8\xi_1+\frac{9}{16}\xi_1^2\right)+\frac{a\pi^4D_{22}}{12b^3}(3+8\xi_1+3\xi_1^2)\right.\\&\quad+\frac{\pi^4m^2}{6ab}(D_{12}+D_{66})\left(3+8\xi_1+\frac{a\pi^4D_{22}}{b^3}\xi_1^2\right)\\&\quad\left.-\sigma t\frac{b\pi^2m^2}{12a}\left(3+8\xi_1+\frac{9}{16}\xi_1^2\right)\right]q_1=0\end{aligned} \tag{26}$$

where the following adimensional parameters are defined:

$$\xi_1=\frac{GJ^*b}{D_{22}}\left(\frac{m}{a}\right)^2 \tag{27}$$

$$\xi_2=\frac{48+320\xi_1+48\pi^2\xi_1^2}{48+128\xi_1+9\pi^2\xi_1^2} \tag{28}$$

$$\xi_3=\frac{96+256\xi_1+24\pi^2\xi_1^2}{48+128\xi_1+9\pi^2\xi_1^2} \tag{29}$$

Equation (26) is used to obtain the buckling load, which corresponds to the nontrivial solution (i.e., $q_1\neq 0$):

$$\begin{aligned}\sigma_{\text{buck}}=\frac{\pi^2}{t}&\left[\left(\frac{m}{a}\right)^2D_{11}+\left(\frac{a}{m}\right)^2\left(\frac{1}{b}\right)^4D_{22}\xi_2\right.\\&\left.+\left(\frac{1}{b}\right)^2(D_{12}+2D_{66})\xi_3\right]\end{aligned} \tag{30}$$

The buckling stress can be obtained by evaluating Eq. (30) for different numbers of half-waves m in the longitudinal direction and taking the minimum value. It is worth noting that this is the stress on the skin, which is, in general, different from the stress on the stiffeners, due to internal load redistribution. As a result, the total buckling load is given by two terms. The first one is the load acting on the skin, which is simply obtained by integrating the buckling stress given by Eq. (30) over the skin cross section. The second term is the load acting on the stiffeners, which can be derived considering the stiffener axial stiffness and the fact that both the skin and the stiffeners undergo the same displacement. In particular, in buckling conditions the displacement is given by

$$\Delta u_{\text{buck}}=-\sigma_{\text{buck}}ta_{11}a \tag{31}$$

The total load on the stiffened panel is then expressed as

$$P_{\text{buck}}=\sigma_{\text{buck}}Bt+\frac{EA}{L}\Delta u_{\text{buck}} \tag{32}$$

and the prebuckling stiffness can be easily calculated as the ratio between buckling load and buckling displacement:

$$K_{\text{pre}}=\frac{P_{\text{buck}}}{\Delta u_{\text{buck}}} \tag{33}$$

The obtained closed-form solution is compared with that for local buckling of composite panels presented by Mittelstedt [21]. Mittelstedt models the blade stiffener as a plate element and considers simply supported conditions along all four edges, avoiding the fact that bending moments can be exchanged between the skin and the stiffener.

The results of [21] are compared with those obtained applying Eq. (30) and are summarized in Table 2. The maximum percent difference between the two formulations is below 8.5%. The larger difference is obtained in the case of the panel with a stiffener of height equal to 40 mm and a stacking sequence $[0\text{ deg}/90\text{ deg}]_{4s}$, which also corresponds to the stiffener with the highest torsional stiffness.

C. Postbuckling Field for Skin Local Buckling

The postbuckling field is studied in the case of skin buckling considering the portion of the panel between the stiffeners. The

Table 2 Comparison between Eq. (30) and [21] results (skin layup $[0\,\text{deg}/90\,\text{deg}]_{2s}$) for σ_{buck} (N/mm^2)

	Stiffener layup $[0\,\text{deg}/90\,\text{deg}]_{2s}$		$[0\,\text{deg}/90\,\text{deg}]_{3s}$		$[0\,\text{deg}/90\,\text{deg}]_{4s}$	
h, mm	Equation (30)	[21]	Equation (30)	[21]	Equation (30)	[21]
20	6.56	6.52	6.99	7.04	7.73	7.94
30	6.65	6.50	7.28	7.41	8.28	8.83
40	6.75	6.41	7.54	7.60	8.75	9.56

stiffeners are modeled as de Saint-Venant torsion bars, and the panel is considered simply supported along the loaded edges and elastically restrained by the stiffeners along the longitudinal edges, as already done for the evaluation of the buckling load. The procedure is applied to isotropic and composite panels, and a symmetric stacking sequence is assumed in the case of composite materials.

The problem is written in a variational form and is solved applying the method of Ritz. The functional is composed of two terms: the first one, F_{sk}, is related to the skin deflection and the second one, V_{st}, is related to the stiffener torsion. The geometrical imperfections, which are always present in real applications, are introduced in the model because they avoid convergence problems from a numerical point of view.

At first, the term of the functional associated with the skin is written as [29]

$$\begin{aligned}F_{\text{sk}} = &-\frac{1}{2}\int_0^a\int_0^b (a_{11}\chi_{/yy}^2 - 2a_{16}\chi_{/xy}\chi_{/yy} + 2a_{12}\chi_{/xx}\chi_{/yy}\\ &+ a_{66}\chi_{/yx}^2 - 2a_{26}\chi_{/xx}\chi_{/xy} + a_{22}\chi_{/xx}^2)\mathrm{d}x\mathrm{d}y\\ &+\frac{1}{2}\int_0^a\int_0^b (D_{11}w_{/xx}^2 + 4D_{16}w_{/xx}w_{/xy} + 2D_{12}w_{/xx}w_{/yy}\\ &+ 4D_{66}w_{/xy}^2 + 4D_{26}w_{/xy}w_{/yy} + D_{22}w_{/yy}^2)\mathrm{d}x\mathrm{d}y\\ &+\frac{1}{2}\int_0^a\int_0^b (-\sigma t w_{/x}^2 + \chi_{/yy}w_{/x}^2 - 2\chi_{/xy}w_{/x}w_{/y} + \chi_{/xx}w_{/y}^2)\mathrm{d}x\mathrm{d}y\\ &+\int_0^a\int_0^b (\sigma t w_0 w_{/xx} - \chi_{/yy}w_0 w_{/xx} + 2\chi_{/xy}w_0 w_{/xy}\\ &- \chi_{/xx}w_0 w_{/yy})\mathrm{d}x\mathrm{d}y \end{aligned} \tag{34}$$

The first two terms of Eq. (34) represent the membrane and the bending energy of the skin. The third and the fourth terms are not directly related to energy consideration, but are responsible for the coupling between compatibility and equilibrium equations. The term related to the stiffeners strain energy V_{st}, which is given by Eq. (21), has to be added to the functional given by Eq. (34), so that the complete functional to minimize is given by

$$F = F_{\text{sk}} + V_{\text{st}} \tag{35}$$

The out-of-plane displacement is described by the superposition of terms satisfying simply supported and clamped boundary conditions along the transverse edges and of sine terms satisfying simply supported boundary conditions along the longitudinal direction:

$$\begin{aligned}w(x,y) = &\sum_{m=1}^{P}\sum_{n=1}^{Q} q_{mn}^{ss}\sin\frac{m\pi x}{a}\sin\frac{n\pi y}{b}\\ &+\sum_{m=1}^{P} q_m^c\left(1-\cos\frac{2\pi y}{b}\right)\sin\frac{n\pi y}{b}\end{aligned} \tag{36}$$

Imposing the natural conditions given by Eq. (23), Eq. (36) becomes

$$\begin{aligned}w(x,y) = &\sum_{m=1,2,3,\ldots}^{P}\sum_{n=1,3,5,\ldots}^{Q} q_{mn}^{ss}\sin\frac{m\pi x}{a}\left[\sin\frac{n\pi y}{b}\right.\\ &\left.+\left(1-\cos\frac{2\pi y}{b}\right)\frac{GJ^*}{4D_{22}}\frac{b\pi}{a^2}m^2 n\right]\end{aligned} \tag{37}$$

The Airy stress function $\chi(x,y)$ can be represented by a trigonometric series of cosines:

$$\chi(x,y) = \sum_{m=0,2,4,\ldots}^{R}\sum_{n=0,2,4,\ldots}^{S}\mu_{mn}\cos\frac{m\pi x}{a}\cos\frac{n\pi y}{b} \tag{38}$$

where the amplitude of the constant term is forced to be null (i.e., $\mu_{00}=0$).

The geometrical imperfections are introduced in the model considering a series of sines:

$$w_0(x,y) = \sum_{m=1}^{T}\sum_{n=1}^{U} d_{mn}\sin\frac{m\pi x}{a}\sin\frac{n\pi y}{b} \tag{39}$$

where the amplitudes d_{mn} are known quantities.

After substitution of the expressions given by Eqs. (37–39) into the functional given by Eq. (35),

$$\begin{aligned}F = &\sum_{rsmn}^{RSRS}\widetilde{A1}_{rsmn}\mu_{rs}\mu_{mn} + \sum_{rsmn}^{PQPQ}(\widetilde{A2}_{rsmn}+\widetilde{A7}_{rsmn})q_{rs}q_{mn}\\ &+\sum_{rsmnpq}^{RSPQPQ}\widetilde{A3}_{rsmnpq}\mu_{rs}q_{mn}q_{pq} + \sigma t\sum_{rsmn}^{PQPQ}\widetilde{A4}_{rsmn}q_{rs}q_{mn}\\ &+\sum_{rsmnpq}^{RSPQTU}\widetilde{A5}_{rsmnpq}\mu_{rs}q_{mn}d_{pq} + \sigma t\sum_{rsmn}^{PQTU}\widetilde{A6}_{rsmn}q_{rs}q_{mn} + \end{aligned} \tag{40}$$

where the terms $\widetilde{A1}$, $\widetilde{A2}$, $\widetilde{A3}$, $\widetilde{A4}$, $\widetilde{A5}$, and $\widetilde{A6}$ are multidimensional arrays of numerical coefficients analytically calculated.

The set of governing equations is derived by applying the stationarity of the functional given by Eq. (40). Because μ_{ik} and q_{ik} are the unknowns of the problem, the variational problem is reduced to

$$\begin{cases}\frac{\partial F}{\partial \mu_{ik}} = 0\\ \frac{\partial F}{\partial q_{ik}} = 0\end{cases} \tag{41}$$

The set of nonlinear equations is solved by applying Eq. (41) to the approximate functional given by Eq. (40). In particular, the first $R\times S$ equations represent the compatibility equations and are given by

$$\begin{aligned}&\sum_{rsmn}^{RSRS}AA_{mn}^{rs}\mu_{mn} + \sum_{rsmnpq}^{RSPQPQ}CC_{mnpq}^{rs}q_{mn}q_{pq}\\ &+\sum_{rsmnpq}^{RSPQTU}CC0_{mnpq}^{rs}q_{mn}d_{pq} = 0\end{aligned} \tag{42}$$

The second $P\times Q$ equations represent the equilibrium conditions and are given by

$$\sum_{rsmn}^{PQPQ} BB^{rs}_{mn} q_{mn} + \sum_{rsmnpq}^{PQPQPQ} DD^{rs}_{mnpq} q_{mn} \mu_{pq} + \sum_{rsmnpq}^{PQTURS} DD0^{rs}_{mnpq} d_{mn} \mu_{pq} + \sum_{rsmn}^{PQPQ} EE^{rs}_{mn} \sigma t q_{mn} + \sum_{rsmn}^{PQTU} EE0^{rs}_{mn} \sigma t d_{mn} = 0 \tag{43}$$

where the terms AA^{rs}_{mn}, BB^{rs}_{mn}, CC^{rs}_{mnpq}, $CC0^{rs}_{mnpq}$, DD^{rs}_{mnpq}, $DD0^{rs}_{mnpq}$, EE^{rs}_{mn}, and $EE0^{rs}_{mn}$ are arrays of numerical coefficients of dimensions 4 and 6.

The governing equations (42) and (43) must now be solved to obtain the force-displacement curve and the postbuckling stiffness. Even if the equations are analytically obtained, a numerical solution is required, due to the nonlinearity of the problem and to the involved number of unknowns. In particular, the method of Newton–Raphson is used. The load history is divided into small steps. Starting from the unloaded condition, the load steps are progressively applied, and the unknowns μ_{ik} and q_{ik} are calculated at each step until the convergence is reached.

The expression of the panel displacement in the case of symmetric laminate is calculated as

$$\Delta u = \frac{1}{b}\int_0^a \int_0^b \left(a_{11}\chi_{/yy} - a_{16}\chi_{/xy} + a_{12}\chi_{/xx} - a_{11}\sigma t - \frac{1}{2} w^2_{/x} + w_0 w_{/xx} \right) \mathrm{d}x\, \mathrm{d}y \tag{44}$$

which is the nonlinear counterpart of Eq. (31), including the effect of the geometrical imperfections.

After substituting Eqs. (37–39) into Eq. (44), the expression for the panel displacement as a function of the unknowns is obtained:

$$\Delta u = -\sigma t a_{11} a + \sum_{rsmn}^{PQPQ} GG_{rsmn} q_{rs} q_{mn} + \sum_{rsmn}^{PQTU} GG0_{rsmn} q_{rs} d_{mn} \tag{45}$$

At the end of the procedure, the total load on the stiffened panel is calculated as is done in the linearized case and hence the force-displacement curve can be traced.

III. Optimization Module

The second part of the fast tool is given by the optimization module. It can implement different optimization algorithms and can be used to optimize different objective functions with or without constraints. Without loss of generality, the optimization can be written as a minimization in the form

$$\begin{cases} \text{Minimize} & f(X) \\ \text{Subject to} & X_i > X_i^{\text{ref}} \end{cases} \tag{46}$$

where f is a general objective function, written in terms of the design variables X. A maximization problem can be written in the form of Eq. (46) by treating the objective function as the inverse of $f(\{X\})$. Common optimization problems include the minimization of the structural weight or the maximization of the buckling loads.

The approach used to handle the constraints is to write an unconstrained problem by means of penalty functions. The normalized violation of the generic ith constraint is expressed as

$$\Delta X_i = (X_i^{\text{ref}} - X_i)/X_i^{\text{ref}} \tag{47}$$

where the normalization is done with respect to a reference value X_i^{ref}. This is motivated by the fact that different constraints can be imposed in the procedure, but the value of the violation must be independent of the type of the considered constraint.

The penalty functions are written as exponential:

$$\eta_i = \begin{cases} e^{\Delta X_i} & \text{if } \Delta X_i > 0 \\ 1 & \text{if } \Delta X_i \le 0 \end{cases} \tag{48}$$

The optimization problem given by Eq. (46) is written as

$$\text{Minimize } f_{\text{un}}(X) = f(X) \prod_{i=1}^{Nc} \eta_i \tag{49}$$

Genetic algorithms are then considered to solve the optimization procedure. This choice is motivated by the ability of genetic algorithms to handle discrete variables and to work in the context of nonconvex design spaces. As genetic algorithms are based on the survival of the fittest individuals, it is common to write the optimization problem in terms of maximization of a fitness function rather than in terms of minimization of an objective function. The generic unconstrained minimization problem given by Eq. (49) is so rewritten as a maximization problem by introducing the fitness function:

$$\text{Maximize } \text{fit}(X) = \frac{1}{f(X)} \frac{1}{\prod_{i=1}^{Nc} \eta_i} \tag{50}$$

Genetic algorithms are implemented using selection, crossover, and mutation operators. In particular, the procedure starts with the generation of an initial population, randomly created inside the design space. The population is then ranked according to the fitness values of each individual, and the fittest members are selected. Among these, the better-performing individuals are passed intact to the following generation: this strategy is referred to as elitism. The other members are created using the crossover and mutation operators.

The procedure can end according to different criteria, such as the maximum number of generations, the change in the average value of the fitness function, or the variance of the fitness value.

IV. Optimization of Two Stiffened Panels

This tool is applied here to perform the minimum weight optimization of a flat isotropic panel and a flat composite panel subjected to axial compression. The optimization scheme is shown in Fig. 7.

At first, the optimization domain is presented describing the design space and the design variables considered in the two cases. Then the optimization strategy is discussed, writing the fitness function in terms of the design variables and describing the constraints that regard both the buckling load and the postbuckling behavior.

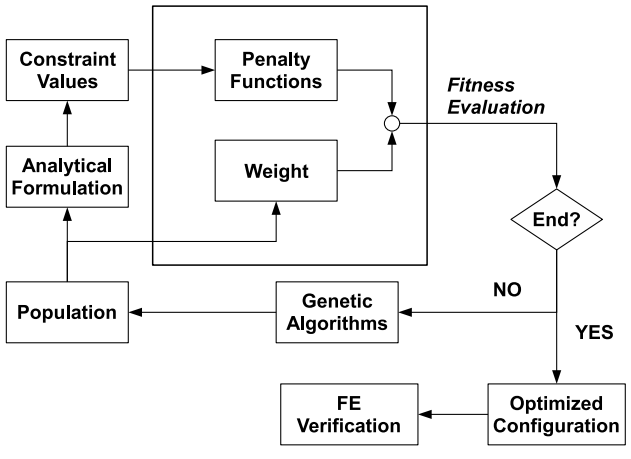

Fig. 7 Optimization scheme (FE denotes finite element).

A. Panels Description and Optimization Domain

Two panels are considered: an isotropic panel and a composite panel. The two panels have widths of 700 mm and lengths of 700 mm. The design variables are the number and the height of the stiffeners as well as the skin and stiffener thicknesses. The stiffeners are considered blade-shaped with heights varying from 22 to 35 mm. The distance between two stiffeners can vary from 140 to 350 mm, depending on the number of the stiffeners, which varies from three to six. In particular, two stiffeners are placed at the edges to avoid local free-edge skin buckling of the external portions.

The considered materials are aluminum alloy 2024-T3 and a graphite/epoxy woven, for which the mechanical properties are reported in Tables 1 and 3, respectively. Table 4 reports the maximum stresses and strains for the graphite/epoxy.

The design variables related to the skin and stiffener thicknesses are chosen according to the considered material.

In the case of isotropic material, the thicknesses are directly the design variables, the skin thickness can vary from 1 to 2.5 mm, and the web thickness can vary from 2 to 6.5 mm, considering discrete steps of 0.50 mm in both cases. The optimization domain of the isotropic panel is shown in Table 5.

In the case of composite material, the design variables are the number of plies. Because of practical design considerations, the angles of orientation of skin and stiffener are limited to 0, ± 45, and 90 deg. According to industrial requirements, the skin is characterized by two external plies oriented at 0 deg; in both cases, the internal plies vary between 1 and 4 and can assume angles of ± 45 deg with the constraint of symmetric layup. The stiffeners are composed of a number of plies between 4 and 12, which are alternatively oriented at 0 and 90 deg. The total thicknesses of the skin and of the stiffener are determined by the number of plies and vary between 0.99 and 2.31 mm and between 1.98 and 6.60 mm, respectively. Table 6 reports the optimization domain of the composite panel.

Table 3 Graphite/epoxy ply mechanical properties

Material properties	Graphite/epoxy ply
Young's modulus E_{11}, N/mm^2	58,615
Young's modulus E_{22}, N/mm^2	58,615
Shear modulus G_{12}, N/mm^2	3,064
Poisson's ratio ν_{12}	0.048
Density ρ, kg/m^3	1510
Ply thickness, mm	0.33

Table 4 Maximum stresses and strains for the graphite/epoxy ply

Property	Value
S_1^T, S_2^T, MPa	440
S_1^C, S_2^C, MPa	468
S_{12}, MPa	99
ϵ_1^T, ϵ_2^T	0.0075
ϵ_1^C, ϵ_2^C	0.0080
γ_{12}^S	0.0323

Table 5 Optimization domain: isotropic panel

Description	Variable	Minimum value	Maximum value
Skin thickness, mm	X_1	1.00	2.50
Stiffener web thickness, mm	X_2	2.00	6.50
Side dimensions of the stiffeners, mm	X_3	22	35
Number of stiffeners	X_4	3	6

Table 6 Optimization domain: composite panel

Description	Variable	Minimum value	Maximum value
Number of layers at ± 45 deg in the skin	X_1	1	4
Number of layers in the stiffeners	X_2	4	12
Side dimensions of the stiffeners	X_3	22	35
Number of stiffeners	X_4	3	6

B. Optimization Scheme

In the examples presented, the goal of the optimization is to minimize the weight, taking into account constraints on the buckling load and on the postbuckling behavior. In particular, the constraints are given by the buckling load and the prebuckling and postbuckling stiffnesses. All of them must be higher than minimum fixed values. Moreover, it is imposed that the optimal configuration undergoes a local buckling mode, and this is done requiring that the ratio between global and local buckling loads is greater than 1.5. With reference to Eq. (46), the optimization problem is formulated as

$$\text{Minimize } W(X)$$
$$\text{Subject to } \begin{cases} P_{\text{buck loc}} > P_{\text{buck loc}}^{\text{ref}} \\ K_{\text{pre}} > K_{\text{pre}}^{\text{ref}} \\ K_{\text{post}} > K_{\text{post}}^{\text{ref}} \\ P_{\text{buck glob}} > 1.5 P_{\text{buck loc}} \end{cases} \tag{51}$$

The panel weight can be easily written as a function of the design variables reported in Tables 5 and 6. For the isotropic panel, the weight is given by

$$W(X_1, X_2, X_3, X_4) = \rho a [B X_1 + X_2 X_3 X_4] \tag{52}$$

In both cases, for the composite panel, it is given by

$$W(X_1, X_2, X_3, X_4) = \rho a t_{\text{ply}} [B(X_1 + 2) + X_2 X_3 X_4] \tag{53}$$

As shown in Fig. 7, the constraint values are evaluated by means of the analytical formulation. The first constraint regards the local buckling load and is evaluated referring to Eq. (32). The prebuckling stiffness constitutes the second constraint and is calculated using Eq. (33).

The third constraint is represented by the postbuckling stiffness. In this case, the force-displacement curve is obtained by solving the nonlinear problem described by Eqs. (42) and (43). In particular, the panel is loaded with a displacement control until a value equal to 3 times the displacement associated with the buckling load, which is given by Eq. (31). Then a linear approximation is performed connecting the last point of the curve with the point corresponding to the buckling condition to derive the postbuckling stiffness.

The fourth constraint regards the buckling mode, as it imposes that the global buckling load is 1.5 times higher than the local buckling load. The global and local buckling loads are evaluated referring to Eqs. (19) and (32). As previously discussed, the constrained problem is transformed into an unconstrained problem and the fitness function results are composed of two terms. The first one is due to the objective function, which coincides with the panel weight. The second one is due to the penalty functions, as can be seen in Fig. 7. The fitness function is therefore given by

$$\text{fit} = \frac{W^{\text{ref}}}{W} \prod_{i=1}^{4} \eta_i \tag{54}$$

where the panel weight is normalized, introducing a reference value W^{ref}. The solution is terminated when the maximum number of generation is reached. Therefore, after calculating the fitness function, the optimization can continue if the maximum number of generations has yet to be reached. In this case, a new population is

Table 7 Optimized isotropic panel with a weight of 27.94 N

	Constraint	Fast tool	Finite element	% diff.
Buckling load, kN	65.00	64.45	59.70	8.84
Prebuckling stiffness, kN/mm	100.00	152.04	152.04	0.00
Postbuckling stiffness, kN/mm	75.00	83.00	83.80	−0.95
Global–local ratio	1.50	1.62	1.82	−10.99

Table 8 Optimized composite panel with a weight of 19.82 N

	Constraint	Fast tool	Finite element	% diff.
Buckling load, kN	65.00	65.16	62.29	4.62
Prebuckling stiffness, kN/mm	100.00	123.82	123.82	0.00
Postbuckling stiffness, kN/mm	75.00	86.13	83.76	2.87
Global–local ratio	1.50	1.55	1.62	−4.32

created and the iteration is repeated. On the other hand, if the maximum number of generations is reached, the procedure is interrupted and the optimized configuration is then obtained as the best individual of the last generation. At the end of the optimization, a finite element analysis is performed to verify the accuracy of the analytical results and to check that no failure occurs.

V. Results

The results obtained by the minimum weight optimizations of the isotropic panel and of the composite panel are presented here. The constraints considered in the optimization are reported in the second columns of Tables 7 and 8, respectively.

An initial population of 30 individuals, generated randomly into the optimization domain, is considered. Good convergence to the optimal solutions is found using a percent of elite children equal to 0.10, a crossover probability of 0.90, and a mutation probability of 0.10. The maximum number of generations is taken equal to 20. The fitness value assumed by the best individual of each generation until the maximum number of generations is shown in Fig. 8.

For the isotropic panel, the best individual of the first generation has a fitness function equal to 0.49. The solution converges to an optimal configuration with a fitness function of 0.64 and a corresponding weight of 27.94 N. It is characterized by skin thickness equal to 1.50 mm, web thickness equal to 2.50 mm, and six stiffeners of height equal to 28.00 mm. It can be observed from Table 7 that the constraint on the buckling load is slightly violated and the three remaining constraints are respected. Indeed, the analytical buckling load is 0.85% lower than the corresponding constraint, but the obtained configuration is the one with the highest fitness function, despite the violation and the consequent nonnull term in the penalty function.

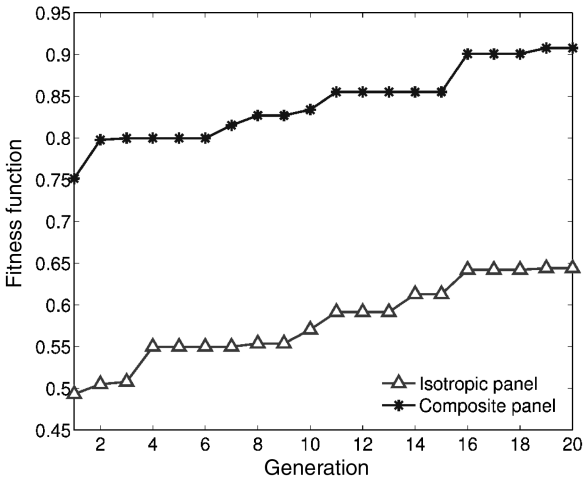

Fig. 8 Convergence of the optimization procedure.

For the composite panel, the best individual of the first generation has a fitness function equal to 0.75. The procedure converges to an optimal configuration characterized by a fitness function of 0.91 and a corresponding weight of 19.83 N. The optimized panel has six stiffeners of height equal to 25.50 mm and is characterized by a skin layup given by [0 deg /45 deg / − 45 deg /45 deg /0 deg] for a total thickness of 1.65 mm. The stiffeners are composed of 15 layers for a total thickness of 4.95 mm. It can be observed from Table 8 that the analytical results respect the four constraints and that the weight is 29% lower than the weight of the isotropic panel.

The constraint on the buckling load is the most critical one for both optimized configurations, as shown in Tables 7 and 8. Indeed, the optimal solutions of the considered design space are close to the boundaries represented by the buckling load value.

The optimized configurations are then verified by finite element analyses using the commercial code ABAQUS [30]. The numerical models are realized using S4R shell elements and choosing the mesh size according to a convergence analysis. The isotropic panel results are composed of 12,400 elements and the composite panel has 13,640 elements, with element dimensions of about 7×7 mm.

The comparison between the numerical and analytical results is reported in Tables 7 and 8, in which the percent differences are also shown, taking the finite element results as reference. The local and global buckling loads are computed by performing linearized eigenvalue analyses. The analytical buckling loads are higher than the numerical ones in both cases, with percent differences below 9%.

Figure 9 shows the local and global buckling modes for the optimized isotropic panel obtained with ABAQUS eigenvalue analysis. The first buckling mode is of local type. The global mode is associated with the 48th eigenvalue. The numerical global buckling load is equal to 108.65 kN and the analytical one is 104.41 kN, resulting in a 3.90% lower analytical value.

Figure 10 shows the local and global buckling modes for the optimized composite panel obtained with ABAQUS eigenvalue analysis. Even in this case, the first buckling mode is of local type. The global mode is associated with the 55th eigenvalue. The numerical global buckling load is equal to 100.84 kN and the analytical one is 101.22 kN, resulting in a 0.37% higher analytical value.

The prebuckling and postbuckling stiffnesses are derived performing nonlinear analyses. The prebuckling stiffness is derived from the slope of the force-displacement curve in the prebuckling range; in both cases, the postbuckling stiffness is obtained as done with the analytical procedure. The comparison between the analytical and numerical pre- and postbuckling stiffnesses for the two analyzed panels is reported in Tables 7 and 8. The analytical prebuckling stiffness coincides with the numerical one in both cases. The comparison with the postbuckling stiffness also shows good agreement between analytical and numerical results, as the percent differences are below 3%. However, it must be noted that for the isotropic panel, the numerical model has a higher postbuckling stiffness than the analytical one, whereas it is the opposite for the composite panel. Good agreement in the postbuckling field is also revealed by the comparison between the force-displacement curves, which are reported in Figs. 11a and 11b.

The nonlinear finite element analyses are also used to verify that no failure occurs in the considered postbuckling field. In the case of isotropic material, it is verified that the von Mises stress does not exceed the material yielding stress, and in the case of composite material, it is applied to a first ply failure criterion based on maximum strain.

Figure 12 shows the contour of the von Mises stress for the optimized isotropic panel at the maximum displacement $\Delta u =$ 1.27 mm. The maximum von Mises stress is equal to 306.40 MPa, which is approximately 10% lower than the material yield stress.

Figure 13 shows the contour of the maximum strain failure index for the optimized composite panel at the maximum displacement $\Delta u = 1.61$ mm. The maximum value of the index is equal to 0.48,

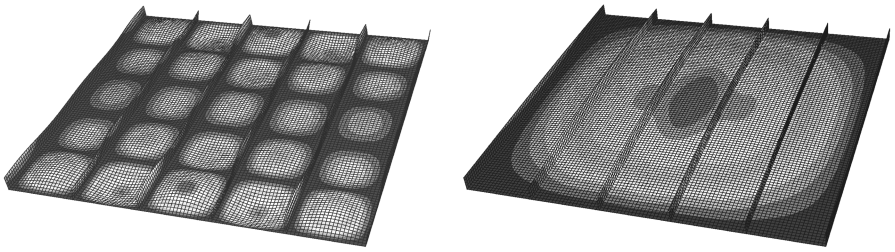

a) Local b) Global

Fig. 9 Buckling modes: isotropic panel.

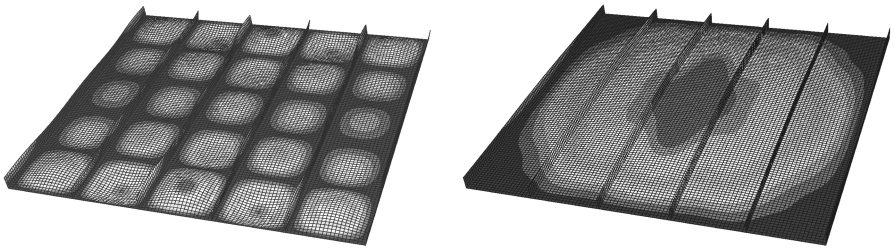

a) Local b) Global

Fig. 10 Buckling mode: composite panel.

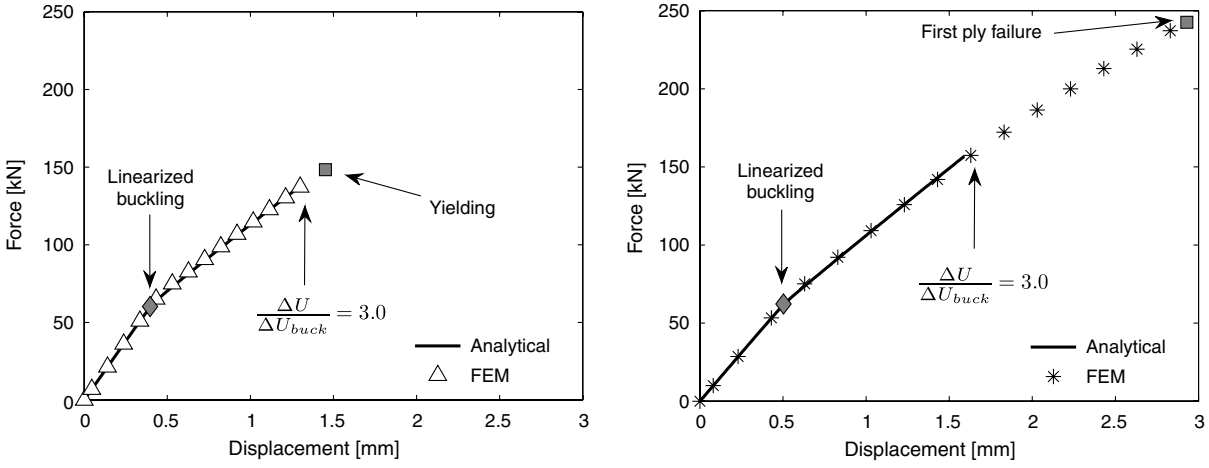

a) Isotropic panel b) Composite panel

Fig. 11 Force-displacement curves (FEM denotes finite element method).

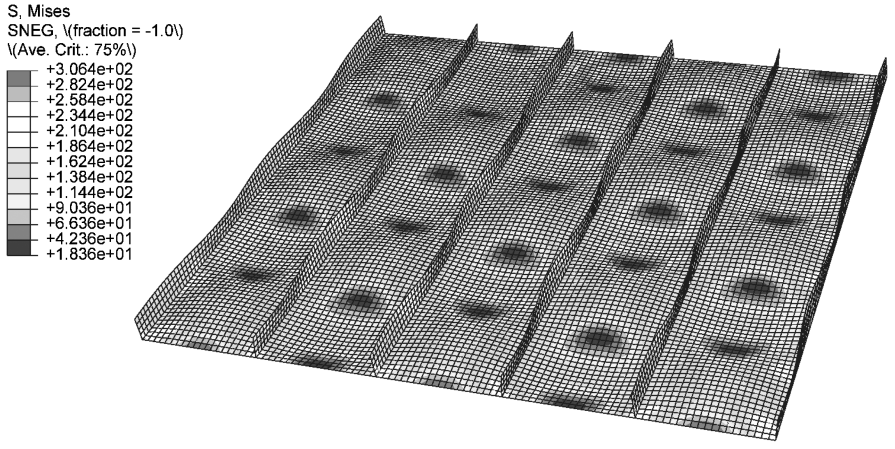

Fig. 12 Contour of von Mises stress at $\Delta u = 1.27$ mm: isotropic panel.

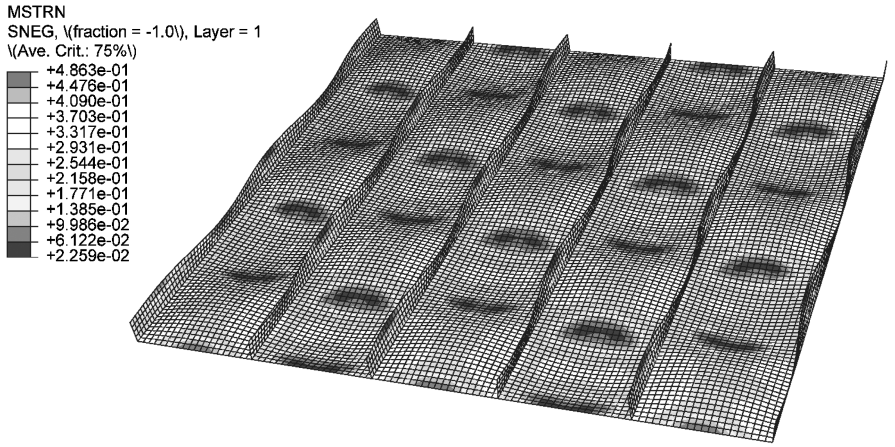

Fig. 13 Contour of maximum strain failure index at $\Delta u = 1.61$ mm: composite panel.

and the first ply failure is expected to happen for the index equal to 1.00.

Each panel optimization required a total of 600 fitness evaluations. Using the presented analytical formulation, the average CPU time to perform the required fitness evaluations in the two considered cases was 274 s on a Core2 Duo 3.00 GHz with 2 GB of RAM. Adding the average CPU time required by the final finite element analysis equal to 382 s, the total CPU time needed to complete the optimization procedure was 656 s. The estimated time of an analogous optimization procedure based only on the use of the finite element method would require an analysis time of about 3690 h. In both cases, it should also be noted that the time required to set up the finite element models in this last case should be equal to the number of evaluations required by the procedure.

VI. Conclusions

A fast tool for the buckling analysis and optimization of stiffened panels made of isotropic and composite materials and subjected to axial compression has been presented. The tool consists of two independent modules: one for the analysis and one for the optimization.

The analysis is performed by implementing an analytical formulation and allows the evaluation of the buckling and postbuckling behavior. The accuracy of the analytical formulation was shown by the comparison with ABAQUS analyses. For the considered examples, it was observed that the analytical local and global buckling loads are higher than the numerical ones, with a difference of 9% or less. Good accuracy was also obtained for the postbuckling stiffnesses, with percent differences below 3%.

Because of the nonconvexity of the design space and the presence of noninteger variables, the optimization was performed using genetic algorithms. The number of fitness evaluations required by genetic algorithms is easily handled by the analysis module. The fitness function, the constraint values, and the optimization algorithm can be easily modified according to industrial requirements, as the fast tool is realized by two independent modules. In the considered examples, buckling and postbuckling requirements were taken into account, but any type of constraint (such as static, dynamic, or cost) can be easily introduced without any change in the overall structure of the tool.

The proposed approach also has the advantage of reduced computational time, which is achieved by implementing the analytical formulation in the analysis module, resulting in a much faster time than an equivalent module based on conventional finite element analysis. This aspect is especially important when the nonlinear behavior in the postbuckling field is taken into account.

The idea of coupling analytical formulations with optimization algorithms seems an effective strategy to enable the designers to consider buckling and postbuckling requirements in the preliminary design phases when detailed information about the structure are not yet available and the design space is too large to consider the use of finite element analysis in a convenient time.

Acknowledgments

The authors wish to express their gratitude to Vittorio Giavotto for valuable discussions and helpful suggestions, particularly on the analytical formulation. His exceptional experience and continuous support made this work possible.

References

[1] Bushnell, D., "PANDA2—Program for Minimum Weight Design of Stiffened, Composite, Locally Buckled Panels," *Computers and Structures*, Vol. 25, No. 4, 1987, pp. 469–605. doi:10.1016/0045-7949(87)90267-7

[2] Butler, R., "Optimum Design of Composite Stiffened Wing Panels—A Parametric Study," *The Aeronautical Journal*, Vol. 99, No. 985, 1995, pp. 169–177.

[3] Goldberg, D. E., *Genetic Algorithms in Search, Optimization and Machine Learning*, Addison Wesley, London, 1989.

[4] Nagendra, S., Haftka, R. T., and Gürdal, Z., "Design of a Blade Stiffened Composite Panel by a Genetic Algorithm Approach," *AIAA/ASME/ASCE/AHS/ASC Structures, 34th SDM Conference*, AIAA, Reston, VA, April 1993, pp. 2418–2436.

[5] Nagendra, S., Jestin, D., Gürdal, Z., Haftka, R. T., and Watson, L. T., "Improved Genetic Algorithm for the Design of Stiffened Composite Panels," *Computers and Structures*, Vol. 58, No. 3, 1996, pp. 543–555. doi:10.1016/0045-7949(95)00160-I

[6] Kang, J. H., and Kim, C. G., "Minimum-Weight Design of Compressively Loaded Composite Plates and Stiffened Panels for Postbuckling Strength by Genetic Algorithm," *Composite Structures*, Vol. 69, No. 2, 2005, pp. 239–246. doi:10.1016/j.compstruct.2004.07.001

[7] Faggiani, A., and Falzon, B. G., "Optimization Strategy for Minimizing Damage in Postbuckling Stiffened Panels," *AIAA Journal*, Vol. 45, No. 10, 2007, pp. 2520–2528. doi:10.2514/1.26910

[8] Bisagni, C., and Lanzi, L., "Post-Buckling Optimisation of Composite Stiffened Panels Using Neural Networks," *Composite Structures*, Vol. 58, No. 2, 2002, pp. 237–247. doi:10.1016/S0263-8223(02)00053-3

[9] Lanzi, L., and Giavotto, V., "Post-Buckling Optimization of Composite Stiffened Panels: Computations and Experiments," *Composite Structures*, Vol. 73, No. 2, 2006, pp. 208–220. doi:10.1016/j.compstruct.2005.11.047

[10] Rikards, R., Abramovich, H., Kalnins, K., and Auzins, J., "Surrogate Modeling in Design Optimization of Stiffened Composite Shells," *Composite Structures*, Vol. 73, No. 2, 2006, pp. 244–251. doi:10.1016/j.compstruct.2005.11.046

[11] Herencia, J. E., Weaver, P. M., and Friswell, M. I., "Optimization of Long Anisotropic Laminated Fiber Composite Panels with T-Shaped Stiffeners," *AIAA Journal*, Vol. 45, No. 10, 2007, pp. 2497–2509. doi:10.2514/1.26321

[12] Jaunky, N., Knight, N. F., Jr., and Ambur, D. R., "Optimal Design of Grid-Stiffened Composite Panels Using Global and Local Buckling Analyses," *Journal of Aircraft*, Vol. 35, No. 3, 1998, pp. 478–486. doi:10.2514/2.2321

[13] Baruch, M., and Singer, J., "Effect of Eccentricity of Stiffeners on the General Instability of Stiffened Cylindrical Shells Under Hydrostatic

Pressure," *Journal of Mechanical Engineering Science*, Vol. 5, No. 1, 1963, pp. 23–27.
doi:10.1243/JMES_JOUR_1963_005_005_02

[14] Block, D. L., Card, M. F., and Mikulas, M. M., "Buckling of Eccentrically Stiffened Orthotropic Cylinders," NASA TN D-2960, 1965.

[15] Simitses, G. J., "General Instability of Eccentrically Stiffened Cylindrical Panels," *Journal of Aircraft*, Vol. 8, No. 7, 1971, pp. 569–575.
doi:10.2514/3.44285

[16] Timoshenko, S. P., and Gere, J. M., *Theory of Elastic Stability*, McGraw–Hill, New York, 1961.

[17] Lekhnitskii, S. G., *Anisotropic Plates*, Gordon and Breach, New York, 1968.

[18] Pevzner, P., Abramovich, H., and Weller, T., "Calculation of the Collapse Load of an Axially Compressed Laminated Composite Stringer-Stiffened Curved Panel-An Engineering Approach," *Composite Structures*, Vol. 83, No. 4, 2008, pp. 341–353.
doi:10.1016/j.compstruct.2007.05.001

[19] Paik, J. K., and Thayamballi, A. K., "Buckling Strength of Steel Plating with Elastically Restrained Edges," *Thin-Walled Structures*, Vol. 37, No. 1, 2000, pp. 27–55.
doi:10.1016/S0263-8231(00)00009-4

[20] Fujikubo, M., and Yao, T., "Elastic Local Buckling Strength of Stiffened Plate Considering Plate/Stiffener Interaction and Welding Residual Stress," *Marine Structures*, Vol. 12, Nos. 9–10, 1999, pp. 543–564.
doi:10.1016/S0951-8339(99)00032-5

[21] Mittelstedt, C., "Closed-Form Analysis of the Buckling Loads of Uniaxially Loaded Blade-Stringer-Stiffened Composite Plates Considering Periodic Boundary Conditions," *Thin-Walled Structures*, Vol. 45, No. 4, 2007, pp. 371–382.
doi:10.1016/j.tws.2007.04.005

[22] Byklum, E., and Amdahl, J., "A Simplified Method for Elastic Large Deflection Analysis of Plates and Stiffened Panels due to Local Buckling," *Thin-Walled Structures*, Vol. 40, No. 11, 2002, pp. 925–953.
doi:10.1016/S0263-8231(02)00042-3

[23] Buermann, P., Rolfes, R., Tessmer, J., and Schagerl, M., "A Semi-Analytical Model for Local Post-Buckling Analysis of Stringer- and Frame-Stiffened Cylindrical Panels," *Thin-Walled Structures*, Vol. 44, No. 1, 2006, pp. 102–114.
doi:10.1016/j.tws.2005.08.010

[24] Romeo, G., and Frulla, G., "Post-Buckling Behaviour of Graphite/Epoxy Stiffened Panels with Initial Imperfections Subjected to Eccentric Biaxial Compression Loading," *International Journal of Non-Linear Mechanics*, Vol. 32, No. 6, 1997, pp. 1017–1033.
doi:10.1016/S0020-7462(96)00136-9

[25] Bisagni, C., "An Analytical Formulation for the Prediction of Buckling and Post-Buckling of Composite Panels and Shells," *Computational Fluid and Solid Mechanics*, Massachusetts Inst. of Technology, Cambridge, MA, 2005, pp. 83–87.

[26] Sheinman, I., and Frostig, Y., "Post-Buckling Analysis of Stiffened Laminated Panel," *Journal of Applied Mechanics*, Vol. 55, No. 3, 1988, pp. 635–640.
doi:10.1115/1.3125841

[27] Young, R. D., Hyer, M. W., and Starnes, J. H., Jr., "Prebuckling and Postbuckling Response of Tailored Composite Stiffened Panels with Axial-Shear Coupling," *41st AIAA/ASME/ASCE/AHS/ASC Structures, Structural Dynamics and Materials*, AIAA, Reston, VA, April 2000, pp. 1–15.

[28] Bisagni, C., and Vescovini, R., "Analytical Formulation for Local Buckling and Post-Buckling Analysis of Stiffened Laminated Panels," *Thin-Walled Structures*, Vol. 47, No. 3, 2009, pp. 318–334.
doi:10.1016/j.tws.2008.07.006

[29] Giavotto, V., "Sulla Meccanica dei Pannelli Anisotropi ed Eterogenei," *Memorie dell'Istituto Lombardo Accademia di Scienzee Lettere*, Vol. 25, No. 5, 1969 (in Italian).

[30] ABAQUS, 6.5, Software Package, Ver. 6.5, Hibbitt, Karlsson & Sorensen, Providence, RI, 2005.